Coadsorption of Hydrogen and Ethylene, and Carbon Monoxide and Ethylene on the Ru(001) Surface

M. M. Hills, J. E. Parmeter,† and W. H. Weinberg*

Contribution from the Division of Chemistry and Chemical Engineering, California Institute of Technology, Pasadena, California 91125. *Received June 25, 1986*

Abstract: A detailed investigation of the coadsorption of ethylene with both preadsorbed hydrogen and preadsorbed carbon monoxide on the Ru(001) surface is reported here. Both preadsorbed hydrogen and carbon monoxide reduce the saturation coverage of subsequently chemisorbed ethylene. The coadsorption of hydrogen with ethylene results in detectable hydrogenation of ethylene to ethane below 250 K, whereas no self-hydrogenation of ethylene to ethane is observed. High-resolution electron energy loss spectra show that ethylene coadsorbed with either hydrogen or carbon monoxide decomposes to ethylidyne (CCH_3) and acetylide (CCH), as it does on the clean surface. Carbon monoxide preadsorption enhances the stability of the ethylidyne such that it decomposes at approximately 420 K, rather than 355 K as on the initially clean Ru(001) surface. Preadsorbed carbon monoxide also reduces the ratio of ethylidyne to acetylide that is formed from ethylene, compared to the ratio observed from an equivalent coverage of ethylene on the clean surface; hydrogen preadsorption, on the other hand, increases this ratio.

I. Introduction

Surprisingly little spectroscopic information is available concerning the interaction of either hydrogen or carbon monoxide with ethylene on well-characterized, single crystalline transition metal surfaces, although much insight regarding the hydrogenation and dehydrogenation of ethylene can be obtained from these measurements. Ratajczykowa and Szymerska[1] have employed mass spectrometry under ultrahigh vacuum (UHV) conditions to investigate the coadsorption of ethylene, hydrogen, and carbon monoxide on Pd(111) between 300 and 330 K, temperatures at which molecularly adsorbed ethylene and ethylidyne (CCH_3) coexist on the clean surface.[2] The relative rates of ethylene hydrogenation and dehydrogenation were compared as functions of hydrogen and carbon monoxide coverage. It was found that the coverage of carbon monoxide controlled the hydrogen coverage, which governed the rate of ethylene hydrogenation relative to ethylene dehydrogenation.

Self-hydrogenation of ethylene to ethane on the Pt(111) surface has been reported by Godbey et al.[3] The maximum rate of ethane formation occurs at 300 K, and this is reduced to 250 K in the presence of preadsorbed hydrogen. Coadsorption of deuterium with ethylene led to the evolution of all isotopically labeled ethane molecules ($C_2H_xD_{6-x}$; x = 0, 1, ..., 6).

Isotopic exchange between deuterium adatoms and the ethylidyne that is formed from the thermal decomposition of ethylene has been studied on the Pt(111) and Rh(111) surfaces.[4,5] Using static secondary ion mass spectrometry and thermal desorption mass spectrometry, Ogle and White have estimated that this exchange reaction on Pt(111) has an activation barrier of approximately 7 kcal/mol.[4] Using electron energy loss spectroscopy (EELS), Koel et al.[5] found that deuterium incorporation into ethylidyne on Rh(111) at 350 K was slow in the sense that significant isotopic exchange was observed only after a few minutes following exposure of ethylidyne to 1 atm of deuterium, and they postulated the existence of an ethylidene ($CDCH_3$) intermediate in the exchange reaction. In neither investigation was ethylidyne directly observed to be hydrogenated to either ethylidene, ethylene, or ethane.

The coadsorption of hydrogen and ethylene on ruthenium is of particular interest because of the high reactivity of this metal for ethylene hydrogenation and its selectivity in the hydrogenation of monosubstituted olefins.[6] Only rhodium is a more active catalyst than ruthenium for ethylene hydrogenation. Knowledge of the interactions of ethylene and hydrogen on the Ru(001) surface will not only clarify the nature of the hydrogenation reaction of ethylene, but it will also allow important comparisons to the interactions of ethylene and hydrogen on Pt(111) and Rh(111) surfaces, each of which has hexagonal symmetry. The interaction between carbon monoxide and ethylene on ruthenium provides information concerning the effects of a nonreactive coadsorbate on the adsorption, desorption, and dehydrogenation of ethylene. This investigation will also complement previous results for ethylene, acetylene, and acetylene plus hydrogen on the Ru(001) surface.[7-10]

To understand the interactions of hydrogen and carbon monoxide with ethylene on the Ru(001) surface, it is necessary first to understand the interaction of hydrogen, carbon monoxide, and ethylene separately with the clean surface. Hydrogen adsorbs dissociatively in threefold hollow sites on the Ru(001) surface producing weak electron energy loss peaks at 845 and 1115 cm^{-1} at saturation coverage.[11] Thermal desorption spectra of hydrogen exhibit two peaks at high surface coverages, which result from interactions among the adatoms rather than the occupation of geometrically inequivalent surface sites.[12] The high-temperature peak appears first at low coverages with a maximum rate of desorption which downshifts from 450 to 380 K with increasing coverage. The low-temperature peak appears at fractional surface coverages exceeding 0.35, with a maximum rate of desorption occurring near 325 K. The saturation fractional coverage is estimated to be 0.85 ± 0.15.[12]

Carbon monoxide adsorbs molecularly on Ru(001) with a single carbon–oxygen stretching frequency which shifts from 1980 to 2060 cm^{-1} as the coverage increases.[13,14] Under no circumstances has CO been observed to dissociate on the clean surface under UHV conditions. A $(\sqrt{3} \times \sqrt{3})R30°$-CO low-energy electron diffraction (LEED) pattern is formed with an optimal fractional surface coverage of 1/3. For this and lower coverages, the magnitude of the carbon–oxygen stretching frequency suggests

† AT&T Bell Laboratories predoctoral fellow.

(1) Ratajczykowa, I.; Szymerska, I. *Chem. Phys. Lett.* **1983**, *96*, 243.
(2) Gates, J. A.; Kesmodel, L. L. *Surf. Sci.* **1986**, *120*, L461.
(3) Godbey, D.; Zaera, F.; Yeates, R.; Somorjai, G. A. *Surf. Sci.* **1986**, *167*, 150.
(4) Ogle, K. M.; White, J. M. *Surf. Sci.* **1986**, *165*, 234.
(5) Koel, B. E.; Bent, B. E.; Somorjai, G. A. *Surf. Sci.* **1984**, *146*, 211.
(6) Boudart, M.; McDonald, M. A. *J. Phys. Chem.* **1984**, *88*, 2185. Henrici-Olive, G.; Olive, S. *Angew. Chem., Int. Ed. Engl.* **1976**, *15*, 136. Dixit, R. S.; Tavlarides, L. L. *Ind. Eng. Chem., Process Des. Dev.* **1983**, *22*, 1.
(7) Hills, M. M.; Parmeter, J. E.; Mullins, C. B.; Weinberg, W. H. *J. Am. Chem. Soc.*, **1986**, *108*, 3554.
(8) Parmeter, J. E.; Hills, M. M.; Weinberg, W. H. *J. Am. Chem. Soc.* **1986**, *108*, 3563.
(9) Parmeter, J. E.; Hills, M. M.; Weinberg, W. H. *J. Am. Chem. Soc.* **1986**, *108*, 3563.
(10) Barteau, M. A.; Broughton, J. Q.; Menzel, D. *Appl. Surf. Sci.* **1984**, *19*, 92.
(11) Barteau, M. A.; Broughton, J. Q.; Menzel, D. *Surf. Sci.* **1983**, *133*, 443.
(12) Shimizu, H.; Christmann, K.; Ertl, G. *J. Catal.* **1980**, *61*, 412.
(13) Thomas, G. E.; Weinberg, W. H. *J. Chem. Phys.* **1979**, *70*, 1437.
(14) Pfnür, H.; Menzel, D.; Hoffmann, F. M.; Ortega, A.; Bradshaw, A. M. *Surf. Sci.* **1980**, *93*, 431.

0002-7863/86/1508-7215$01.50/0

that the CO is adsorbed in on-top sites. The observation of bridging CO on this surface has not been reported previously. Michalk and co-workers[15] have confirmed the on-top site symmetry of the $(\sqrt{3} \times \sqrt{3})R30°$ overlayer with dynamical LEED calculations. They found also that the CO is adsorbed essentially perpendicularly to the Ru(001) surface with a ruthenium–carbon bond length of 2.0 ± 0.1 Å and a carbon–oxygen bond length of 1.10 ± 0.1 Å. The fractional CO coverage at saturation is 0.65, where a $(5\sqrt{3} \times 5\sqrt{3})R30°$ coincidence LEED pattern, presumably due to a compressed CO overlayer, is observed.[13] Two peaks are observed in the thermal desorption spectra of CO.[16] The high-temperature peak has a maximum desorption rate at approximately 480 K, while the low-temperature peak, which is present at fractional coverages exceeding 1/3, has a maximum rate of desorption near 410 K.

The interaction of ethylene with the clean Ru(001) surface has been discussed in detail recently.[7] To summarize, below 150 K ethylene is chemisorbed molecularly in a di-σ-bonded configuration. Competing molecular desorption and dehydrogenation of the di-σ-bonded ethylene to ethylidyne, acetylide (CCH), and hydrogen adatoms occur between 150 and 250 K. As shown by near-edge X-ray absorption fine structure and LEED calculations, the ethylidyne on Pt(111) is adsorbed in threefold hollow sites.[17,18] This suggests that the ethylidyne adsorbed on Ru(001) also adsorbs in these sites. The ethylidyne on Ru(001) dehydrogenates completely to hydrogen adatoms and either carbon dimers or carbon adatoms with no spectroscopically observable, partially dehydrogenated intermediates.[7] The hydrogen desorbs in a sharp peak at 355 K with a shoulder near 420 K for a saturation coverage of chemisorbed ethylene. Cleavage of the carbon–carbon bond of the acetylide, which yields methylidyne (CH) and surface carbon, is observed at 380 K. Reaction-limited hydrogen desorption occurs between 500 and 700 K as the methylidyne dehydrogenates.

Peebles et al.[19] have shown that preadsorption of carbon monoxide suppresses the high-temperature thermal desorption peak of postadsorbed hydrogen on the Ru(001) surface. The lower temperature thermal desorption peak of hydrogen both decreases in intensity and shifts to lower temperature (from approximately 325 to 305 K) with increasing carbon monoxide coverage.[20] Although it is not known whether these observations are the result of lateral H–CO repulsive interactions giving rise to the formation of high-density islands of hydrogen adatoms in the presence of carbon monoxide or a weakening of the Ru–H bond due to the presence of the coadsorbed carbon monoxide, the former explanation was shown to be correct by a LEED investigation of the coadsorption of hydrogen and CO on Rh(111), where nearly complete segregation of the two species was observed on the surface.[21]

These observations raise several questions. First, how do preadsorbed hydrogen and carbon monoxide affect the subsequent adsorption of ethylene? Second, is the thermal decomposition of ethylene altered by the presence of hydrogen or carbon monoxide, and, if so, how? For example, are ethylidyne and acetylide formed, and, if so, in the same relative concentrations? Finally, can ethylene hydrogenation to ethane be observed under UHV conditions when hydrogen and ethylene are coadsorbed?

II. Experimental Procedures

Thermal desorption mass spectrometry experiments were conducted in a UHV apparatus which has been described in detail previously.[22,23]

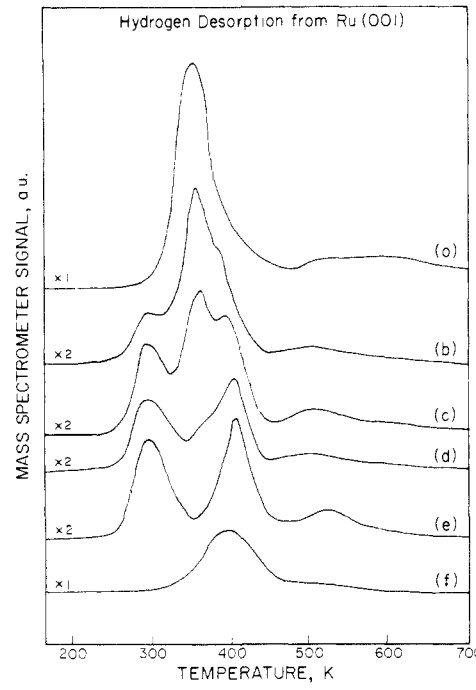

Figure 1. Thermal desorption spectra of hydrogen after C_2H_4 adsorption on the clean and CO precovered Ru(001) surface at 130 K: (a) 1 langmuir of C_2H_4; (b) 0.4 langmuir of CO followed by 1 langmuir of C_2H_4; (c) 0.6 langmuir of CO followed by 1 langmuir of of C_2H_4; (d) 0.8 langmuir of CO followed by 1 langmuir of of C_2H_4; (e) 1.0 langmuir of CO followed by 1 langmuir of of C_2H_4; (f) 0.4 langmuir of C_2H_4.

Briefly, the chamber is pumped by both a 220-L/s noble ion pump and a titanium sublimation pump, which reduce the base pressure below 10^{-10} torr. The crystal is cooled to below 100 K using liquid nitrogen. Linear heating rates of 5–20 K/s are achieved via resistive heating, controlled by a power supply interfaced to an LSI-11 DEC laboratory computer. This UHV chamber contains a UTI-100C quadrupole mass spectrometer enclosed in a glass envelope for selective sampling of gases that desorb from only the well-oriented front surface of the single crystal.[24] Low-energy electron diffraction optics and a rotatable Faraday cup are available for the display of LEED patterns and the measurement of LEED beam profiles. A single-pass cylindrical mirror electron energy analyzer with an integral electron gun is available for Auger electron spectroscopy.

A second UHV chamber was used to conduct high-resolution electron energy loss spectroscopic experiments. This chamber also has a base pressure below 10^{-10} torr using similar pumping techniques; liquid nitrogen cooling and resistive heating of the crystal were similarly employed. The home-built Kuyatt-Simpson-Type EEL spectrometer is described in detail elsewhere.[25,26] It was operated such that the kinetic energy of the electron beam incident upon the crystal was approximately 4 eV at an angle of incidence of 60° with respect to the surface normal. The spectra were measured with a resolution of 60–80 cm^{-1} (full-width at half-maximum of the elastically scattered peak), while maintaining a count rate of $1.5–3 \times 10^5$ counts/s in the elastic channel. This UHV chamber also contains a quadrupole mass spectrometer, but it was not, in general employed in the thermal desorption measurements reported here.

The techniques used for orienting, cutting, polishing, and mounting the Ru(001) crystals have been described previously.[25,26] The crystals were cleaned using periodic argon ion sputtering and routine annealing to 1000 K in 7×10^{-8} torr of O_2, followed by annealing to 1700 K in vacuo. Surface cleanliness was monitored in the two UHV chambers by Auger electron spectroscopy, EELS, and hydrogen thermal desorption.

Research purity (99.9995% min) hydrogen, CP grade (99.5%) deuterium and ethylene, and research purity (99.99% min) carbon monoxide were obtained from Matheson. The ethylene was purified further by three freeze–thaw–pump cycles. Research purity (99.99%) ethylene-d_4

(15) Michalk, G.; Moritz, W.; Pfnür, H.; Menzel, D. *Surf. Sci.* **1983**, *129*, 92.
(16) Pfnür, H.; Feulner, P.; Menzel, D. *J. Chem. Phys.* **1983**, *79*, 2400, 4613.
(17) Horsley, J. A.; Stöhr, J.; Koestner, R. J. *J. Chem. Phys.* **1985**, *83*, 3146.
(18) Koestner, R. J.; Van Hove, M. A.; Somorjai, G. A. *J. Phys. Chem.* **1983**, *87*, 203.
(19) Peebles, D. E.; Schreifels, J. A.; White, J. M. *Surf. Sci.* **1982**, *116*, 117.
(20) These results were confirmed independently in our laboratory.
(21) Williams, E. D.; Thiel, P. A.; Weinberg, W. H.; Yates, J. T., Jr. *J. Chem. Phys.* **1980**, *72*, 3496.
(22) Williams, E. D; Weinberg, W. H. *Surf. Sci.* **1979**, *82*, 93.
(23) Williams, E. D.; Weinberg, W. H. *J. Vac. Sci. Technol.* **1982**, *20*, 534.
(24) Feulner, P.; Menzel, D. *J. Vac. Sci. Technol.* **1980**, *17*, 662.
(25) Thomas, G. E.; Weinberg, W. H. *Phys. Rev. Lett.* **1978**, *41*, 1181.
(26) Thomas, G. E.; Weinberg, W. H. *Rev. Sci. Instrum.* **1979**, *50*, 497.

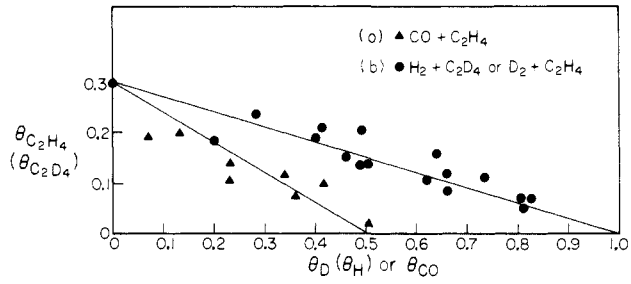

Figure 2. Inhibition of ethylene adsorption by deuterium (hydrogen) or CO precoverages: (a) fractional coverage of chemisorbed C_2H_4 as a function of CO precoverage; (b) fractional coverage of chemisorbed C_2H_4 (C_2D_4) as a function of deuterium (hydrogen) precoverage.

was purchased from Merck and Co. The purity of all gases was verified in situ by mass spectrometry in both UHV chambers.

III. Results

A. Coadsorption of Carbon Monoxide and Ethylene. Preadsorbed CO alters significantly the thermal desorption spectra of hydrogen from adsorbed ethylene on Ru(001). Figure 1a shows the hydrogen thermal desorption spectrum following a saturation exposure of 1 langmuir of C_2H_4 (1 langmuir ≡ 10^{-6} torr·s) at 130 K, while Figure 1b–e shows a series of hydrogen thermal desorption spectra for various preexposures of carbon monoxide, followed by a constant ethylene exposure of 1 langmuir at 130 K (at which temperature no multilayer of ethylene forms). Figure 1f shows the hydrogen thermal desorption spectrum following the adsorption of 0.4 langmuir of ethylene on the clean surface. As the precoverage of CO increases, new desorption peaks of hydrogen appear at 290 and 420 K, while the 355-K peak decreases in intensity, disappearing completely at CO exposures of 1 langmuir or more. In addition, the high-temperature tail (above 480 K) shifts to lower temperature, and the total amount of hydrogen that desorbs decreases with increasing carbon monoxide coverage.

The inhibition in the chemisorption of ethylene by preadsorbed CO ($\theta_{C_2H_4}$ vs. θ_{CO}) is illustrated in Figure 2a, where $\theta_{C_2H_4}$ includes both the reversibly and irreversibly *chemisorbed* ethylene. This relationship was derived from the data of Figure 1, together with the corresponding thermal desorption spectra of molecular ethylene. In the presence of CO, approximately 20% of the chemisorbed ethylene desorbs molecularly, as is observed also on the clean surface. Displacement of CO by ethylene was not observed. However, for all CO precoverages the thermal desorption peaks of CO coadsorbed with ethylene are downshifted by approximately 20 K with respect to the desorption of equivalent coverages of CO from the otherwise clean Ru(001) surface.

The preadsorption of 0.4 langmuir ($\theta_{C_2H_4} \approx 0.13$) of ethylene, followed by 2 langmuir of carbon monoxide ($\theta_{CO} \approx 0.20$), produced hydrogen thermal desorption spectra similar to Figure 1c. Greater initial ethylene coverages blocked carbon monoxide adsorption to a larger extent, and the preadsorption of 1 langmuir of ethylene followed by any exposure of CO resulted in H_2 and C_2H_4 thermal desorption spectra that were nearly identical with those of ethylene adsorbed on the clean Ru(001) surface.

Electron energy loss spectra for various precoverages of carbon monoxide followed by an exposure of ethylene at 80 K are similar to those of ethylene adsorbed on the clean surface. As on the clean Ru(001) surface, multilayers of ethylene condense at 80 K. Annealing the crystal to 110 K desorbs this multilayer, leaving an overlayer composed of carbon monoxide and di-σ-bonded ethylene. Figure 3a shows an EEL spectrum measured after annealing a saturation coverage of ethylene adsorbed on the clean Ru(001) surface to 110 K and is indicative of di-σ-bonded ethylene. The mode assignments for this di-σ-bonded ethylene are discussed in detail elsewhere.[7] Briefly, di-σ-bonded ethylene on Ru(001) produces strong CH_2 twisting and wagging modes at 900 and 1145 cm^{-1} and a symmetric carbon–hydrogen stretching mode at 2940 cm^{-1}, which reflect the rehybridization of the carbon atoms in ethylene to nearly sp^3. Additional energy loss features at 460, 650, 775, 1040, 1450, and 3050 cm^{-1} are due respectively

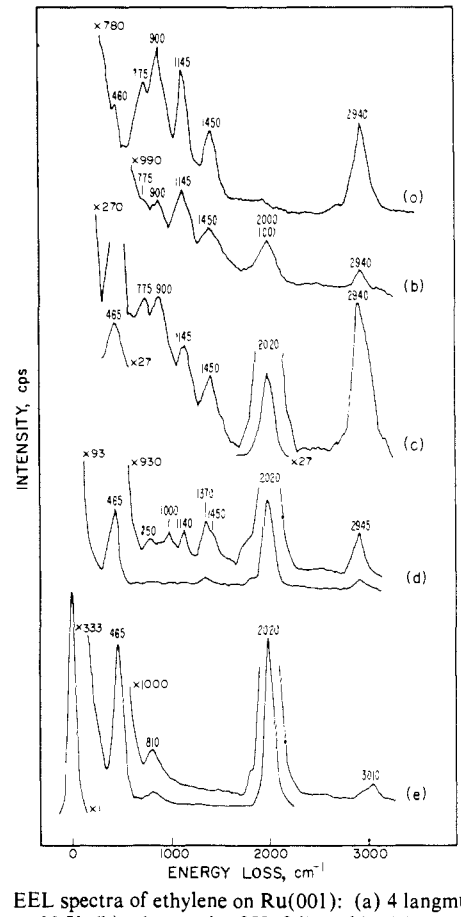

Figure 3. EEL spectra of ethylene on Ru(001): (a) 4 langmuir of C_2H_4 annealed to 120 K; (b) 1 langmuir of H_2 followed by 1 langmuir of C_2H_4 annealed to 120 K; (c) 0.6 langmuir of CO followed by 1 langmuir of C_2H_4 annealed to 120 K; (d) 0.6 langmuir of CO followed by 1 langmuir of C_2H_4 annealed to 280 K; (e) 0.6 langmuir of CO followed by 1 langmuir of C_2H_4 annealed to 400 K.

to the symmetric and asymmetric carbon–ruthenium stretching modes, the CH_2 rocking mode, the carbon–carbon stretching mode, the CH_2 scissoring mode, and the asymmetric carbon–hydrogen stretching mode of the molecularly chemisorbed ethylene. Although not all of these modes are resolved in Figure 3a, they have been assigned from other EEL spectra.

Figure 3c is an EEL spectrum measured following an exposure of 0.6 langmuir of CO ($\theta_{CO} = 0.33$) and then 1 langmuir of C_2H_4 ($\theta_{C_2H_4} = 0.08$–0.09) at 80 K with subsequent annealing to 110 K. (Figure 3b is an EEL spectrum measured following an exposure of 1 langmuir of H_2 and then 1 langmuir of C_2H_4, and will be discussed in section IIIB.) The mixed overlayer of Figure 3c consists of di-σ-bonded C_2H_4 and linearly bonded CO. The modes of both ethylene and carbon monoxide are unchanged compared to those observed when ethylene and carbon monoxide are adsorbed separately on the Ru(001) surface. The symmetric Ru—CO stretching mode and the C≡O stretching mode are observed at 465 and 2020 cm^{-1} in Figure 3c. All mode assignments of ethylene coadsorbed with carbon monoxide were confirmed by EEL spectra of CO coadsorbed with deuterated ethylene.

Annealing the mixed overlayer to between 230 and 280 K causes competing desorption and dehydrogenation of the di-σ-bonded ethylene. A subsequently measured EEL spectrum (Figure 3d) indicates the presence of ethylidyne and acetylide, the same decomposition products formed from ethylene that is adsorbed on the clean surface. The ethylidyne is characterized by the ν(CC) mode at 1140 cm^{-1}, the $\delta_s(CH_3)$ mode at 1370 cm^{-1}, the $\rho(CH_3)$ mode at 1000 cm^{-1}, and the $\nu(CH_3)$ mode at 2945 cm^{-1}.[7] Note that ethylidyne produces no losses below 1000 cm^{-1} except for ν_s(Ru-C) at 480 cm^{-1} (which is unresolved from ν(Ru–C) of CO); the loss at 750 cm^{-1} is due to the carbon–hydrogen bending mode of acetylide. In Figure 3d, the carbon–carbon stretching mode of acetylide at 1290 cm^{-1} and the carbon–hydrogen stretching

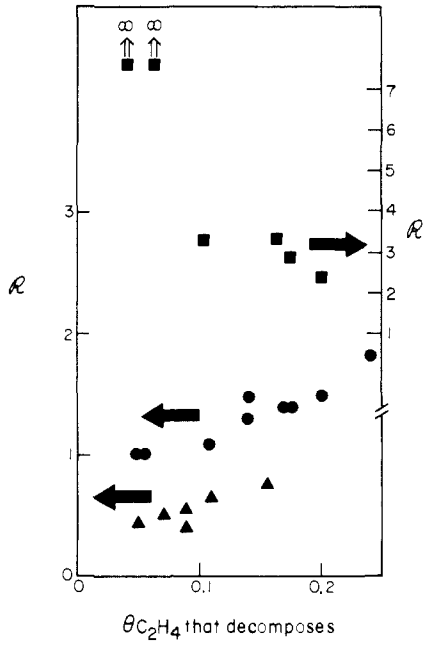

Figure 4. The ratio of ethylidyne to acetylide formed from ethylene (R) as a function of the saturation coverage of irreversibly chemisorbed ethylene for (a, ▲) a mixed CO and ethylene overlayer; (b, ●) ethylene on the clean surface; (c, ■) a hydrogen (deuterium) and C_2D_4 (C_2H_4) overlayer.

mode of acetylide at 2960 cm^{-1} are unresolved from the $\delta_s(CH_3)$ and $\nu(CH_3)$ modes of ethylidyne. This overlayer contains a small concentration of bridging CO in addition to linearly bonded CO, as indicated by the shoulder at 1840 cm^{-1} in Figure 3d.[27] This μ-CO forms near 220 K when acetylide and ethylidyne are formed, and disappears near 450 K as the CO begins to desorb. The CO thermal desorption spectrum of the overlayer corresponding to Figure 3d was virtually identical with that of a CO coverage of 0.33 adsorbed on the clean surface, except downshifted by approximately 20 K. No unusual features were observed which might be attributed to the presence of the bridging CO.

Annealing the surface above 350 K initiates decomposition of the ethylidyne, forming hydrogen adatoms, carbon adatoms, and (possibly) carbon dimers. The hydrogen from ethylidyne decomposition desorbs in either the 355 K or the 420 K thermal desorption peaks (cf. Figure 1), depending upon the CO coverage. Hydrogen thermal desorption spectra have been used to obtain the ratio (R) of ethylidyne to acetylide that is formed from ethylene coadsorbed with CO. This ratio is plotted in Figure 4a as a function of the coverage of the irreversibly chemisorbed ethylene. These data were obtained by exposing the Ru(001) surface to a variable precoverage of CO, followed by a saturation exposure of ethylene. As shown in Figure 4a,b, preadsorbed CO decreases the ratio of ethylidyne to acetylide that is formed from postadsorbed ethylene relative to the ratio observed for an equivalent coverage of ethylene on the clean surface. However, this ratio does increase with increasing ethylene coverages (lower CO precoverages), as it does for ethylene adsorbed on the clean surface. This issue will be discussed in detail in section IV.A.2.

The carbon–carbon bond of the acetylide is cleaved, forming carbon adatoms and methylidyne, when the overlayer is annealed to 400 K. An EEL spectrum of coadsorbed methylidyne and CO is shown in Figure 3e. The characteristic modes of methylidyne are a carbon–hydrogen bending mode at 810 cm^{-1} and a carbon–hydrogen stretching mode at 3010 cm^{-1}. The Ru–CH stretching mode (at 440 cm^{-1}) is obscured by the ν(Ru–CO) mode at 460 cm^{-1}. Annealing to 600 K decomposes all of the methylidyne, desorbing hydrogen and CO, and leaving only surface carbon with ν(Ru–C) at approximately 600 cm^{-1}.

B. Coadsorption of Hydrogen and Ethylene. Electron energy loss spectra of hydrogen and ethylene coadsorbed on Ru(001) are similar to those of ethylene adsorbed on the clean surface with the exception that the modes due to ethylidyne, following annealing to 280 K, are more intense relative to the modes of acetylide. This indicates that the thermal decomposition products of ethylene adsorbed on the clean and the hydrogen-precovered Ru(001) surfaces are the same under our experimental conditions. Figure 3 (a and b) compares respectively the EEL spectrum of a saturation coverage of ethylene adsorbed on the clean surface at 80 K and annealed to 110 K ($\theta_{C_2H_4} = 0.30$) with that of the Ru(001) surface exposed to 1 langmuir of H_2 ($\theta_H = 0.65$) followed by a saturation coverage of ethylene ($\theta_{C_2H_4} = 0.13$) at 80 K and subsequently annealed to 110 K. The spectrum of Figure 3b is less intense because less ethylene is adsorbed. It is apparent, however, that these spectra correspond to the same surface species, namely, di-σ-bonded ethylene. Hydrogen adatoms are also present in the overlayer corresponding to the spectrum of Figure 3b. The weak ruthenium–hydrogen modes, which occur at 780 and 1115 cm^{-1} (at this hydrogen coverage) with an intensity less than 0.04% of the elastic peak,[11] are obscured, however, by losses due to the adsorbed ethylene. A small amount of carbon monoxide is also present in the overlayer corresponding to the spectrum of Figure 3b, as indicated by the presence of the ν(C≡O) mode of CO at 2000 cm^{-1}. The weak intensity of this mode in Figure 3b (cf. Figure 3c–e) implies that the fractional coverage of CO in this overlayer is less than 0.01, and it has no influence on the chemisorption and reaction of hydrogen and ethylene.

Annealing the coadsorbed hydrogen and ethylene overlayer to higher temperatures results in EEL spectra similar to those of ethylene adsorbed on the clean Ru(001) surface. The di-σ-bonded ethylene ($\theta_{C_2H_4} \approx 0.13$) dehydrogenates to ethylidyne and acetylide between 150 and 280 K. The ratio of ethylidyne to acetylide is approximately 2.5, as judged by the areas of the hydrogen thermal desorption peaks of Figure 5b, compared to a branching ratio of 1.3 for a coverage of ethylene of 0.13 on the clean Ru(001) surface. The dependence of the ratio of ethylidyne to acetylide upon the coverage of irreversibly adsorbed ethylene for preadsorbed deuterium (hydrogen) followed by a saturation postexposure of C_2H_4 (C_2D_4) is compared to that observed for ethylene adsorbed on the clean surface in Figure 4b,c. Although there are large uncertainties in the data of Figure 4c because of the small acetylide coverages, the preadsorption of hydrogen clearly results in an increased ratio of ethylidyne to acetylide relative to the ratio observed following the dehydrogenation of an equivalent coverage of ethylene on the clean surface. Indeed, a saturation hydrogen precoverage ($\theta_H \approx 0.85$ and $\theta_{C_2H_4} \approx 0.05$) completely inhibits acetylide formation. The ethylidyne decomposes to carbon (possibly dimers) and hydrogen adatoms below 345 K. Near 400 K the carbon–carbon bond of the acetylide cleaves, forming methylidyne and surface carbon. Finally, the methylidyne decomposes, evolving hydrogen, above 480 K.

The thermal desorption spectra of hydrogen and ethylene coadsorbed on Ru(001) and ethylene adsorbed on the clean surface are somewhat different. Figure 5a illustrates the hydrogen thermal desorption spectrum after 1 langmuir of C_2H_4 is adsorbed on this surface. There is a sharp peak at 345 K, a shoulder near 420 K, and a high-temperature tail extending from 480 to 700 K. Figure 5b shows the hydrogen thermal desorption spectrum after an exposure of 1 langmuir of H_2 followed by 1 langmuir of C_2H_4 at 100 K. This spectrum exhibits a much more prominent shoulder on the high-temperature side of the (sharper) 345 K peak, and the high-temperature tail terminates between 600 and 650 K. As discussed previously,[7] and confirmed by the carbon monoxide and ethylene coadsorption experiments, the 345 K peak of Figure 5a corresponds to desorption of hydrogen limited by ethylidyne decomposition. Because of the similarity of the EEL spectra of ethylene adsorbed on the clean surface and ethylene coadsorbed with hydrogen, the high-temperature tails (above approximately 480 K) of Figure 5a,b correspond to decomposition-limited desorption of hydrogen from the same species, methylidyne.

(27) Approximately 8% based on the intensities of the CO stretching modes of linear and bridge-bonded CO, and assuming that the dipole derivatives of the CO that is bridge bonded and linearly bonded are equal.

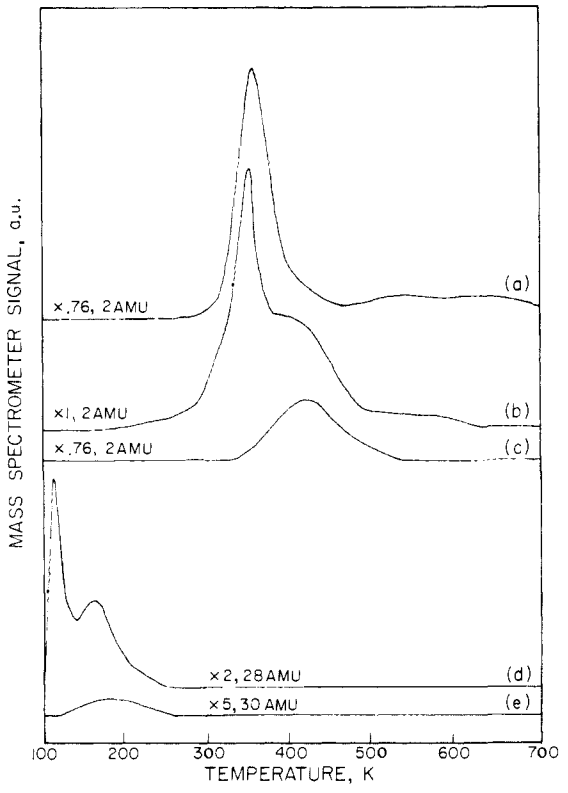

Figure 5. Thermal desorption spectra after C_2H_4 or H_2 adsorption on the clean and hydrogen precovered surfaces at 100 K: (a) H_2 thermal desorption following a 1-langmuir exposure of C_2H_4; (b) H_2 thermal desorption after 1-langmuir exposure of H_2 followed by 1 langmuir of C_2H_4; (c) H_2 thermal desorption following a 0.4-langmuir exposure of H_2; (d) C_2H_4 thermal desorption after a 1-langmuir exposure of H_2 followed by 1 langmuir of C_2H_4; (e) C_2H_6 thermal desorption after a 1-langmuir exposure of H_2 followed by 1 langmuir of C_2H_4.

The shoulder near 420 K in the hydrogen thermal desorption spectrum of coadsorbed hydrogen and ethylene (Figure 5b) is due to desorption-limited hydrogen from the Ru(001) surface. This shoulder occurs at approximately the same temperature at which a similar coverage of hydrogen desorbs from the clean surface, as may be seen in Figure 5c, and the area under the shoulder increases with increasing hydrogen precoverage. Proof that this shoulder corresponds to desorption-limited hydrogen was provided by additional thermal desorption measurements in which the hydrogen and ethylene overlayer was annealed to 800 K, and then the (uncleaned) surface was exposed to hydrogen. The subsequent hydrogen thermal desorption spectrum indicated that the shoulder (now a peak since the 345 K peak was absent) was repopulated, demonstrating that the shoulder of Figure 5b represents desorption-limited hydrogen from the surface. No other hydrogen thermal desorption peaks were observed, implying that no carbon–hydrogen bonds were formed. Complementary EEL spectra measured after annealing the carbon- and hydrogen-covered surface to various temperatures supported the presence of only C(a) and H(a): i.e., no hydrogen-containing species such as CH, CH_2, or CH_3 were observed under any conditions. This disagrees with the results of Barteau et al.[28] who reported the hydrogenation of surface carbon to methylidyne on Ru(001).

In addition to the desorption of hydrogen, annealing the mixed hydrogen and ethylene overlayer resulted in the desorption of ethylene and the formation and desorption of ethane, as shown in Figure 5d,e. Condensed ethylene desorbed in a multilayer peak at 110 K (cf. Figure 5d). Ethane and chemisorbed ethylene desorbed in broad peaks, the tails of which extend to approximately 250 K. The intermediate to ethane formation, presumably ethyl, was not sufficiently stable to be observed spectroscopically by

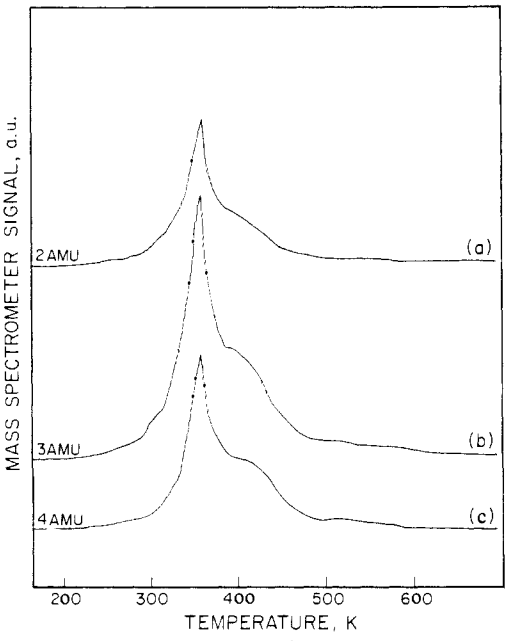

Figure 6. Thermal desorption spectra after a 1-langmuir exposure of D_2 followed by 1 langmuir of C_2H_4 at 130 K: (a) H_2 thermal desorption; (b) HD thermal desorption; (c) D_2 thermal desorption.

EELS. Ethane was formed following fractional precoverages of hydrogen exceeding 0.4 and subsequent saturation exposures of ethylene. The amount of ethane that desorbed corresponds to an effective fractional surface coverage of only approximately 0.01, which is less than one-third of the amount of ethylene which desorbs molecularly. The fraction of chemisorbed ethylene which desorbs molecularly increases from 0.2 to 0.6 as the initial fractional coverage of hydrogen increases from 0 to 0.85.

Thermal desorption measurements of preadsorbed deuterium and postadsorbed ethylene were carried out to examine both the extent of isotopic mixing among the adspecies and the inhibition of ethylene adsorption by deuterium. Considerable isotopic mixing occurred in the desorbed hydrogen (cf. Figure 6). These experiments also showed that within our experimental uncertainty postexposures of 1 langmuir or more of ethylene did not displace any preadsorbed deuterium. Coadsorption of deuterium (hydrogen) with molecularly chemisorbed C_2H_4 (C_2D_4) indicated that isotopic exchange between these two species was slight in that only minor amounts of any ethylene and ethane desorption products except C_2H_4 (C_2D_4) and $C_2H_4D_2$ ($C_2D_4H_2$) were observed.

The results of isotopic exchange experiments between both CCH_3 and CCH and deuterium adatoms are discussed elsewhere.[29] Briefly, electron energy loss spectra of acetylide and ethylidyne formed from C_2H_2 and coadsorbed with deuterium provide evidence for isotopic exchange between deuterium and CCH but no exchange between deuterium and ethylidyne.

Isotope exchange experiments between deuterated methylidyne and postadsorbed hydrogen [and equivalently between CH(a) and D(a)] were also carried out. Deuterated methylidyne (coadsorbed with carbon adatoms) was formed by exposing the Ru(001) surface to 4 langmuir of C_2D_4 at 100 K and annealing to 440 K such that $\theta_C \approx 0.38$ and $\theta_{CD} \approx 0.10$. The surface was then cooled to 100 K, exposed to a saturation coverage of hydrogen ($0.3 \lesssim \theta_H \lesssim 0.4$), and a thermal desorption experiment conducted. Hydrogen, HD, and D_2 were detected in desorption-limited peaks at 400 K, and in tails above 500 K due to dehydrogenation of CH and CD. No other species such as methane were observed to desorb. A comparison of the areas under the high-temperature tails of the H_2, HD, and D_2 thermal desorption spectra shows that 20 to 30% of the deuterated methylidyne underwent isotopic exchange. The observation of deuterium desorption below 400 K indicates that isotopic exchange occurs below this temperature. The occurrence

(28) Barteau, M. A.; Feulner, P.; Stengl, R.; Broughton, J. Q.; Menzel, D. *J. Catal.* **1985**, *94*, 51.

(29) Weinberg, W. H.; Parmeter, J. E.; Hills, M. M., in preparation.

of isotopic exchange between CH coadsorbed with deuterium has also been confirmed with EELS, and is reported elsewhere.[9] These EELS measurements showed no hydrogenation of methylidyne to stable methylene or methyl species.

The extent of inhibition of ethylene adsorption by preadsorbed deuterium was estimated from the H_2, HD, D_2, ethylene, and ethane thermal desorption spectra for various initial surface coverages of deuterium followed by a saturation exposure of ethylene. These data were used to construct Figure 2b, a plot of $\theta_{C_2H_4}$ vs. θ_D, where θ_D was determined from the HD, D_2, and $C_2H_4D_2$ thermal desorption spectra. Clearly, a saturation precoverage of deuterium does not completely inhibit ethylene adsorption. The inhibition of ethylene adsorption by deuterium adatoms is weaker than that by preadsorbed carbon monoxide.

IV. Discussion

A. Coadsorption of Carbon Monoxide and Ethylene. 1. Adsorption. From Figure 1 and the corresponding thermal desorption spectra of molecular ethylene, it was determined that the fraction of the di-σ-bonded ethylene which desorbed molecularly from the CO preexposed and subsequently ethylene *saturated* surface was 20% of the total fractional coverage of chemisorbed ethylene, independent of the CO coverage. This fraction is approximately the same as that observed when a saturated overlayer of ethylene is chemisorbed on the clean Ru(001) surface. This result shows that preadsorbed CO does not inhibit ethylene thermal decomposition on the surface *relative* to molecular desorption. However, preadsorbed CO does inhibit ethylene adsorption, as illustrated in Figure 2.

The approximately linear decrease in the ethylene coverage with carbon monoxide coverage suggests that CO is simply (geometrically) blocking the surface for ethylene adsorption. The reciprocal of the magnitude of the slope of the line in Figure 2a indicates that 1.7 CO admolecules poison the adsorption of one ethylene molecule. Assuming that the areas occupied by a carbon monoxide admolecule and an ethylene admolecule are inversely proportional to the saturation fractional coverages of CO (0.65) and ethylene (0.30), respectively, then 2.2 (i.e., 0.65/0.30) CO admolecules would block adsorption of one ethylene molecule. We observe that fewer CO admolecules are required to block adsorption of one ethylene molecule because ethylene has a significantly lower heat of adsorption than carbon monoxide and, unlike CO, does not form a compressible overlayer.

2. Thermal Decomposition. The results of Peebles et al.[19] and unpublished data from our laboratory indicate that the peak at 290 K in the hydrogen thermal desorption spectra for coadsorbed CO and C_2H_4 (cf. Figure 1b–e) is due to surface hydrogen that desorbs at a slightly lower temperature than does hydrogen coadsorbed with CO for the same coverages of CO and surface hydrogen. This is presumably the result of a higher effective hydrogen density due to the presence of ethylidyne and acetylide. That the peak at 290 K results from desorption-limited hydrogen was confirmed by hydrogen thermal desorption spectra of coadsorbed hydrogen and carbon monoxide on a carbon precovered surface ($\theta_C \approx 0.15$) which showed hydrogen desorption in a single peak at 290 K for fractional coverages of CO exceeding 0.35. From the observed EEL spectra both of ethylene adsorbed on the clean surface[7] and of ethylene coadsorbed with carbon monoxide, it is clear that this surface hydrogen is derived from ethylene dehydrogenation to acetylide and ethylidyne below 250 K.

The peak at 420 K in the hydrogen thermal desorption spectra of Figure 1b–e results from the decomposition of ethylidyne. Without coadsorbed CO, the ethylidyne begins to decompose near 330 K, reaching a maximum rate at 355 K. This is manifest as a rather sharp peak in the hydrogen thermal desorption spectrum at this temperature, as may be seen in Figure 1a. Preadsorbed CO not only decreases the amount of ethylidyne that is formed relative to acetylide (cf. Figure 4), but it also shifts the ethylidyne decomposition to a higher temperature. The *onset* of ethylidyne decomposition in the presence of a fractional coverage of CO of 0.4 occurs at the same temperature (approximately 380 K) at which CO begins to desorb, as shown both by thermal desorption and EELS results. This suggests that CO inhibits ethylidyne decomposition (effectively stabilizing the ethylidyne), e.g., by geometrically blocking the surface adjacent to the ethylidyne that is necessary for its decomposition. Thus as the precoverage of CO is increased, more ethylidyne is prevented from dehydrogenating prior to CO desorption. A fractional surface precoverage of CO exceeding 0.4 prevents any dehydrogenation of the ethylidyne at 355 K.

The final changes in the hydrogen thermal desorption spectra of carbon monoxide coadsorbed with ethylene on Ru(001) are a shift to lower temperature and an increased intensity (*relative* to the 355 and 420 K peaks) of the high-temperature tail above approximately 480 K, which is due to methylidyne decomposition. The former is due to the lower coverage of ethylene on the surface when CO is preadsorbed and is associated with the greater availability of vacant adsites at the temperature of methylidyne decomposition, i.e., a lower concentration of adsorbed carbon.[30] The increasing intensity of the high-temperature tail in the hydrogen thermal desorption spectra, due to methylidyne decomposition, relative to the 355 and 420 K peaks is a consequence of a reduction in ethylidyne formation relative to acetylide formation, as shown in Figure 4. Recall that methylidyne is derived only from acetylide. The enhancement of acetylide formation with increasing CO precoverage also causes the increasing relative intensity of the 290 K peak in the hydrogen thermal desorption spectra since acetylide formation produces two more hydrogen adatoms than does ethylidyne formation, and these two adatoms desorb in the 290 K peak in the presence of CO. The enhanced acetylide formation relative to ethylidyne formation in the presence of CO is obviously greater than that which would be expected due to the lower ethylene surface coverage in the presence of CO (cf. Figure 4). A reasonable explanation for this effect is that the net balance of interaction energies among hydrogen, carbon monoxide, and the intermediate(s) to ethylidyne and acetylide formation is repulsive with respect to the interaction energy which results in the absence of hydrogen. This inhibits the reaction of hydrogen with the precursor to ethylidyne formation and, therefore, favors dehydrogenation to acetylide with respect to ethylidyne formation.[31] This point of view is consistent with the repulsive interactions that occur between coadsorbed hydrogen and CO which result in phase separation of these two species.

Thus the assignment of peaks in the hydrogen thermal desorption spectra is as follows: the β_1 peak at 290 K is composed of surface hydrogen from ethylene dehydrogenation to acetylide and ethylidyne, downshifted by the presence of CO; the γ_1 peak at 355 K is composed of hydrogen from the decomposition of ethylidyne; the γ_2 peak at 420 K is composed of hydrogen from the decomposition of ethylidyne that is stabilized by coadsorbed CO; and the γ_3 peak near 530 K is composed of hydrogen from methylidyne decomposition. These assignments are consistent with the observed ratios of the peak areas. For example, in the case of Figure 1e where no peak at 355 K is observed, the stoichiometry required by the above peak assignments is $\beta_1 = (\gamma_2/3) + 3\gamma_3$. This stoichiometry has been confirmed by the thermal desorption spectrum of Figure 1e, which exhibits relative peak areas for $\beta_1:\gamma_2:\gamma_3$ of 0.55:0.3:0.15. Thus the carbon monoxide–hydrogen repulsive interactions, which cause phase separation and the lower binding energy of surface hydrogen which results in desorption at a lower temperature, allow us to confirm the stoichiometry of the decomposition products of ethylene adsorbed on the Ru(001) surface which were identified by EELS. The ratio of these peaks also confirm that only a small fraction, *if any*, of the ethylidyne decomposes to methylidyne. If we assume that ethylidyne can decompose to methylidyne, then the ratios of the peaks in these

(30) Note that the high-temperature tail in Figure 1d is similar to the tail in the hydrogen thermal desorption spectrum following the adsorption of 0.4 langmuir of C_2H_4 on the clean Ru(001) surface, shown in Figure 1f.

(31) This explanation implies that the precursor to ethylidyne formation is CCH_2. Evidence for the existence of this precursor is provided by the combined results of experiments of coadsorbed ethylene and hydrogen and coadsorbed acetylene and hydrogen. This will be discussed in detail elsewhere.[29]

hydrogen thermal desorption spectra indicate that *at most* 10% of the ethylidyne decomposes to methylidyne.

Finally, we have observed that the adsorption of ethylene also affects the bonding of preadsorbed carbon monoxide. Postadsorption of ethylene induced the formation of a small fraction of bridging carbon monoxide, which is not observed at any coverage of CO on the otherwise clean Ru (001) surface. Furthermore, the presence of carbon and methylidyne following ethylene dehydrogenation reduced the binding energy of preadsorbed carbon monoxide such that the CO desorbed at approximately 20 K below the temperature at which an equivalent fractional coverage of CO desorbs from the clean surface.

B. Coadsorption of Hydrogen and Ethylene. 1. Adsorption. Figure 2b shows that preadsorbed deuterium does not inhibit ethylene adsorption so effectively as does preadsorbed carbon monoxide. The ethylene coverage that is plotted is the fractional coverage of *chemisorbed* ethylene following multilayer desorption. Preadsorbed deuterium decreases the ethylene coverage approximately linearly, and a saturation coverage of deuterium ($\theta_D \approx 0.85$) does not completely block ethylene adsorption. The linear dependence of ethylene coverage upon deuterium precoverage suggests that the deuterium, like preadsorbed carbon monoxide, is geometrically blocking the surface with respect to the subsequent adsorption of ethylene. The results shown in Figure 2b suggest that 3.3 hydrogen adatoms poison the adsorption of one ethylene molecule. As expected, the number of hydrogen atoms required to block the adsorption of one ethylene molecule is greater than the number of carbon monoxide molecules (1.7). The extrapolated intercept of the abscissa of Figure 2b indicates a hydrogen coverage of one adatom per ruthenium unit cell is necessary to poison the surface essentially completely with respect to the subsequent adsorption of ethylene.

2. Thermal Decomposition. The preadsorption of deuterium atoms into the threefold sites on Ru(001) decreases the availability of vacant threefold sites for the products of ethylene decomposition. The ethylene decomposition products, ethylidyne and acetylide, require one and three vacant threefold sites, respectively, for hydrogen adatoms. Thus, as the deuterium precoverage is increased and fewer threefold sites are available, a larger fraction of the chemisorbed ethylene is desorbed molecularly as C_2H_4 or hydrogenated to ethane, compared to chemisorbed ethylene on the otherwise clean Ru(001) surface. The fraction of chemisorbed ethylene which desorbs molecularly as C_2H_4 increases from 0.2 to 0.6 as the fractional hydrogen precoverage increases from 0 to 0.85. The higher concentration of hydrogen (deuterium) adatoms on the surface below 250 K facilitates ethane formation, which was not observed when ethylene was adsorbed on the clean Ru(001) surface. Ethane evolution was observed only in the coverage range $0.4 \lesssim \theta_H$ (preceding a saturation exposure of ethylene), and the ethane that desorbed corresponds to an effective fractional surface coverage of approximately 0.01. We note further than ethane forms via the hydrogenation of di-σ-bonded ethylene and not ethylidyne or acetylide, which are not present on the surface at the temperature at which ethane evolution is initiated.

Thermal desorption experiments of coadsorbed deuterium and C_2H_4 or hydrogen and C_2D_4 showed that the majority ethane species were $C_2D_2H_4$ in the first case and $C_2H_2D_4$ in the latter. The predominant ethylene species that desorbed molecularly from these overlayers were C_2H_4 and C_2D_4, respectively; i.e., very little isotopic mixing with the molecularly adsorbed ethylene occurred. These results suggest that ethane formation occurs via the irreversible addition of two surface hydrogen or deuterium adatoms to ethylene.

Thermal desorption and EEL spectra of deuterium coadsorbed with CH or hydrogen coadsorbed with CD indicated that approximately 20% of the methylidyne underwent isotopic exchange. Similarly, acetylide underwent limited isotopic exchange with surface hydrogen. The mechanisms by which these exchange reactions proceed will be discussed elsewhere.[29] On the other hand, isotopic exchange between surface hydrogen and CCD_3 did not occur. This is in agreement with the results of Koel et al.[5] who identified via EELS an ethylidyne on Rh(111) at 300 K following C_2H_4 adsorption, and H_2 and C_2H_4 coadsorption. This ethylidyne underwent H–D exchange when exposed to deuterium only at high deuterium pressures (1 atm).

As discussed earlier, the 345 K peak in the hydrogen thermal desorption spectra of hydrogen and ethylene coadsorbed on Ru(001) (cf. Figure 5b) corresponds to the desorption of hydrogen that is limited by ethylidyne decomposition. The high-temperature tail, above approximately 480 K, in the spectra corresponds to the reaction-limited desorption of hydrogen from the decomposition of methylidyne which is formed by the cleavage of the carbon–carbon bond of acetylide at 400 K. The observed change in the areas of these two peaks indicates that the ratio of ethylidyne to acetylide increases with hydrogen precoverage, as shown in Figure 4. Indeed, one might expect that an increase in hydrogen or deuterium precoverage would favor ethylidyne over acetylide since the former is composed of two more hydrogen atoms.

As may be seen in Figure 5b, the shoulder at 420 K in the hydrogen thermal desorption spectra of hydrogen and ethylene adsorbed on Ru(001) is enhanced relative to that of hydrogen thermal desorption from ethylene adsorbed on the clean surface. The temperature corresponding to the maximum rate of hydrogen desorption from this shoulder is approximately 20 K lower than that at which an equivalent amount of hydrogen desorbs from the clean Ru(001) surface. However, this shoulder could be repopulated by adsorbing hydrogen on the (uncleaned) surface that results from annealing coadsorbed hydrogen and ethylene to 800 K, which desorbs the hydrogen completely. This indicates that this shoulder corresponds to desorption-limited surface hydrogen.

V. Conclusions

Both preadsorbed carbon monoxide and hydrogen (deuterium) inhibit ethylene postadsorption on the Ru(001) surface. Of the two, carbon monoxide more effectively inhibits ethylene adsorption. The EEL spectra were virtually identical for ethylene adsorbed on Ru(001), ethylene adsorbed with preadsorbed hydrogen, and ethylene adsorbed with preadsorbed carbon monoxide. In all three cases, the ethylene decomposed upon heating to ethylidyne and acetylide. The ethylidyne dehydrogenated completely to carbon and hydrogen adatoms with further heating, while the acetylide underwent carbon–carbon bond cleavage to form carbon adatoms and methylidyne. The preadsorption of CO causes surface hydrogen to desorb at a lower temperature (290 K) and ethylidyne to decompose at a higher temperature (400 K). The observed ratios of peak areas in the hydrogen thermal desorption spectra confirm the identity of the stable ethylene decomposition products, ethylidyne and acetylide, as observed via EELS.

The presence of preadsorbed CO and hydrogen alters the ratio of the ethylene decomposition products, ethylidyne and acetylide. Carbon monoxide preadsorption enhances acetylide formation relative to ethylidyne formation from postadsorbed ethylene, compared to an equivalent coverage of ethylene adsorbed on the clean surface, while hydrogen preadsorption enhances ethylidyne formation, such that a saturation preexposure of hydrogen completely suppresses acetylide formation.

The preadsorption of hydrogen initiated ethane formation and desorption (with a maximum rate at approximately 200 K). The desorption of ethylene and the formation of ethane were enhanced with increasing hydrogen precoverage, compared to the dehydrogenation products, ethylidyne and acetylide.

Acknowledgment. This work was supported by the National Science Foundation under Grant No. CHE-8516615.

Registry No. C_2H_4, 74-85-1; H_2, 1333-74-0; CO, 630-08-0; Ru, 7440-18-8.